Accepted Manuscript

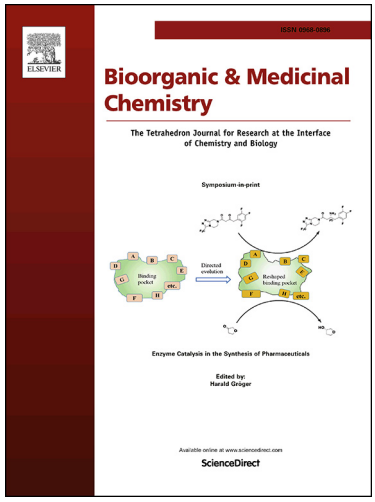

Design, Synthesis, and Biological Evaluation of Novel Oxadiazole- and Thiazole-Based Histamine H_3R Ligands

Mohammad A. Khanfar, David Reiner, Stefanie Hagenow, Holger Stark

PII: S0968-0896(18)30764-8
DOI: https://doi.org/10.1016/j.bmc.2018.06.028
Reference: BMC 14420

To appear in: *Bioorganic & Medicinal Chemistry*

Received Date: 20 April 2018
Revised Date: 8 June 2018
Accepted Date: 20 June 2018

Please cite this article as: Khanfar, M.A., Reiner, D., Hagenow, S., Stark, H., Design, Synthesis, and Biological Evaluation of Novel Oxadiazole- and Thiazole-Based Histamine H_3R Ligands, *Bioorganic & Medicinal Chemistry* (2018), doi: https://doi.org/10.1016/j.bmc.2018.06.028

Design, Synthesis, and Biological Evaluation of Novel Oxadiazole- and Thiazole-Based Histamine H_3R Ligands

Mohammad A. Khanfar[1,2,3], David Reiner[1], Stefanie Hagenow[1], Holger Stark[1*]

[1]Heinrich Heine University Düsseldorf, Institute of Pharmaceutical and Medicinal Chemistry, Universitaetsstr. 1, 40225 Duesseldorf, Germany
[2]Faculty of Pharmacy, University of Jordan, P.O Box 13140, Amman 11942, Jordan.
[3]College of Pharmacy, Alfaisal University, Al Takhassusi Rd, Riyadh, 11533, Saudi Arabia

*Corresponding author: Prof. Holger Stark, Tel.: +49 211 81-10478, Fax: +49 211 81-13359, email: stark@hhu.de

Abstract

Histamine H_3 receptor (H_3R) is largely expressed in the CNS and modulation of the H_3R function can affect histamine synthesis and liberation, and modulate the release of many other neurotransmitters. Targeting H_3R with antagonists/inverse agonists may have therapeutic applications in neurodegenerative disorders, gastrointestinal and inflammatory diseases. This prompted us to design and synthesize azole-based H_3R ligands, i.e. having oxadiazole- or thiazole-based core structures. While ligands of oxadiazole scaffold were almost inactive, thiazole-based ligands were very potent and several exhibited binding affinities in a nanomolar concentration range. Ligands combining 4-cyanophenyl moiety as arbitrary region, *para*-xylene or piperidine carbamoyl linkers, and/or pyrrolidine or piperidine basic heads were found to be the most active within this series of thiazole-based H_3R ligands. The most active ligands were *in silico* screened for ADMET properties and drug-likeness. They fulfilled Lipinski's and Veber's rules and exhibited potential activities for oral administration, blood-brain barrier penetration, low hepatotoxicity, combined with an overall good toxicity profile.

Keywords: histamine; H_3 receptor; ligands; ADMET; thiazole; oxadiazole

1. Introduction

Histamine belongs to biogenic amines, which influence several intracellular pathways, including its neurotransmission activities.[1-4] Histamine's regulatory character in cellular activities is attributed to its binding to four subtypes of G-protein-coupled receptors (GPCRs); H_1, H_2, H_3, and H_4 that are differentially expressed in several cell types.[5, 6]

Histamine H_3 receptor (H_3R) is a member of transmembrane class A of GPCR family.[7, 8] H_3R is largely expressed on the histaminergic neurons of the CNS, located pre- and postsynaptically.[9] It plays an essential role in the biosynthesis and release of histamine as well as in the modulation the release of different neurotransmitters (e.g., dopamine, serotonin, acetylcholine, noradrenaline, GABA, and glutamate.)[10, 11] Peripherally, H_3R is marginally distributed in the peripheral nervous system and regulates the sympathetic effector systems and pain sensation.[12] Consequently, modulation of the H_3R function can potentially affect histaminergic neurotransmission. Therefore, targeting H_3R with antagonists/inverse agonists may have therapeutic applications in neurodegenerative disorders, such as Parkinson's disease, Alzheimer's disease, as well as in depression, epilepsy, schizophrenia and in sleep disorders. [14-19]

Recently, a number of H_3R antagonists/inverse agonists have entered late clinical trials for the treatment of several CNS disorders.[15, 20, 21] In March 2016, the European Medicines Agency authorized marketing of pitolisant (Wakix®) as the first H_3R inverse agonist for the treatment of narcolepsy, designated as an orphan drug since narcolepsy belongs to the rare diseases.[22-24] Pitolisant is also currently in phase III clinical trials for the treatment of hypersomnia.[25]

First H_3R antagonists/inverse agonists reported in literature were imidazole-based compounds followed by non-imidazoles in the next generation. They share a general pharmacophore generated from numerous chemical scaffolds (Figure 1).[15, 26, 27] Prototype H_3R antagonists/inverse agonists pharmacophore consist of basic moiety (mainly tertiary amine electrostatically interacting with Asp114 within H_3R binding site) separated by a spacer to a central core (mainly electron-rich moiety)[28]. The distance between the basic head and the electron rich moiety is approximately 4-5 Å, equivalent to 4 bonds in linear arrangement. The central core is usually connected to an arbitrary region, mainly lipophilic, but polar or basic and even acidic moieties are also tolerable.[29] This arbitrary region modulates potency and pharmacokinetic properties of H_3R antagonists/inverse agonists.[27, 30]

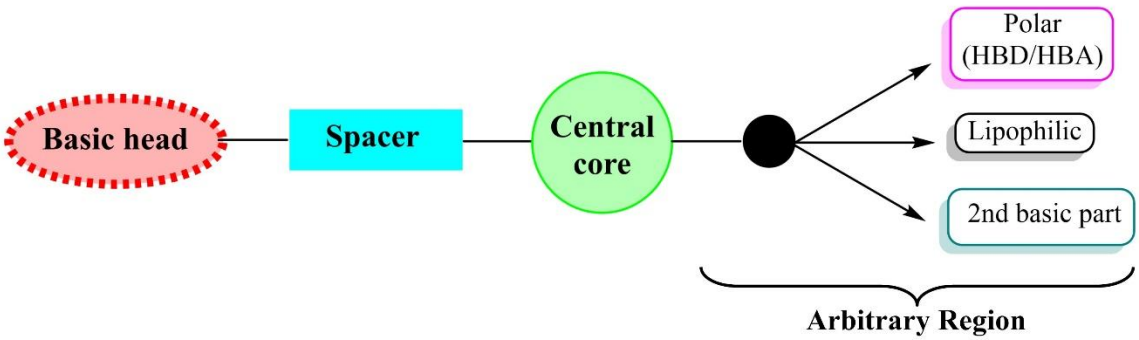

Figure 1. Schematic presentation of the pharmacophore model of H_3R antagonists/inverse agonists.

Oxadiazole and thiazole nuclei have attracted a wide attention in the search for new therapeutic molecules. They are widely exploited in various applications because of their versatile applicability in multiple therapeutic agents and their blood-brain barrier (BBB) permeability;[31, 32] Five-membered heterocycles as core motifs in non-

imidazole H_3R ligands with structural resemblance to the presented structures were explored in earlier research projects resulting in affine compounds (Figure 2).[33, 34] Among them ADS-531 that recently underwent *in vivo* examination upon effects on food-intake and neurotransmitter systems[35, 36] The former progress in the design of potent oxadiazole- and thiazole-based H_3R ligands prompted our research group to explore 2-arylthiazole-4-ylethers as analogues to ST-979 but differing in the arrangement of the substituents.[37] Furthermore, *N*-aryl-1,3,4-oxadiazole-2-amines and 3-phenyl-1,2,4-oxadiazole-5-carboxamides (cf. GSK247246 and ST-1095) were designed to increase structural and linkage diversity in the H_3R central core motif , basically linked to our previous work on variations of polar azole core motifs in H_3R ligands (Figure 2).[37-40] Our synthetic effort combines various aliphatic and aromatic spacers of variable length, and arbitrary region of electronically and sterically variable substituents. Several H_3R analogues with binding affinities in low nanomolar concentrations were obtained within this project.

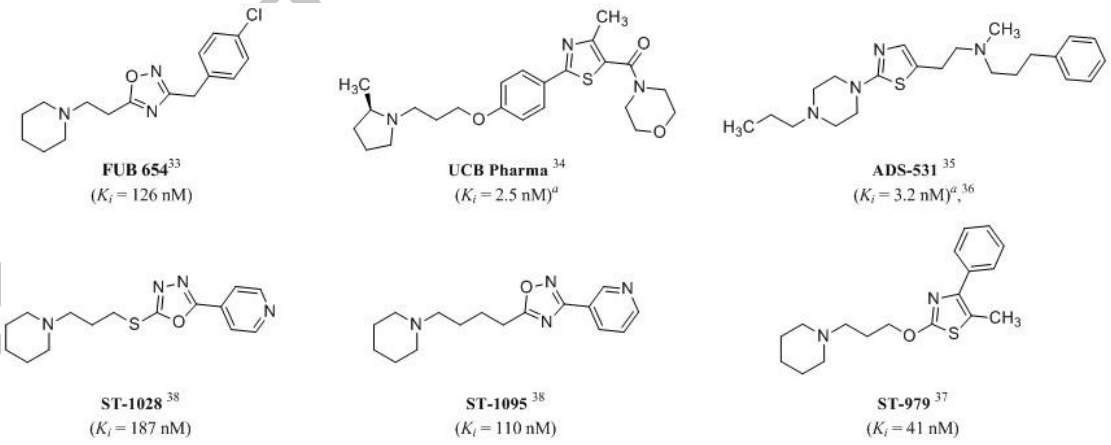

Figure 2. Selected oxadiazole- and thiazole-based H_3 receptor ligands serving as a basis for design of new H_3R ligands [a]K_i values calculated from published pK_i values.

2. Results and Discussions

2.1 Hit-Identification and Hit-to-Lead-Optimization

Synthetic design strategy was driven by an initial structural hypothesis for various azole-based H_3R ligands fitting the H_3R-pharmacophoric map (Figure 1).[37-39] The following structural modification strategies were applied to design potent H_3R ligands: (1) employing oxadiazole (1,2,4 and 1,3,4) or thiazole rings as a polar, electron-rich central core; (2) several cyclic and noncyclic amines were examined as a basic head of the designed H_3R ligands including: pyrrolidine, piperidine, piperazine and noncyclic aliphatic tertiary amines; (3) variable spacers of different chain length connecting the central core and the basic head were examined using aliphatic and aromatic linkers. Linkers of 2 to 5 elements of cyclic or noncyclic structure were tested for optimal length; (4) substituted and unsubstituted aromatic and heteroaromatic rings of variable size and electronic properties were placed on the arbitrary region. Substantial modifications can be conducted on the arbitrary region to modulate potency, solubility and pharmacokinetic properties. Initially, only a few ligands of each compound series without changes in the arbitrary region were synthesized and evaluated for hit identification. Hit-to-lead optimization was conducted for those structures with promising results.

2.2 Chemistry.

An efficient one-pot synthesis of substituted 2-anilino-1,3,4-oxadiazoles was applied. A carboxylic acid (1.0 eq.) and 4-phenyl-3-thiosemicarbazide (1.0 eq.) were mixed in DCM at room temperature with three equivalents of *N*-(3-dimethylaminopropyl)-N^1-ethylcarbodiimide (EDCI) as coupling reagent, producing the corresponding 2-anilino- 1,3,4-oxadiazoles (**2a**-**m**) (Scheme 1). The thiosemicarbazides **1a**-**e** were readily prepared by reacting the corresponding isothiocyanate with hydrazine under reflux in MeOH.

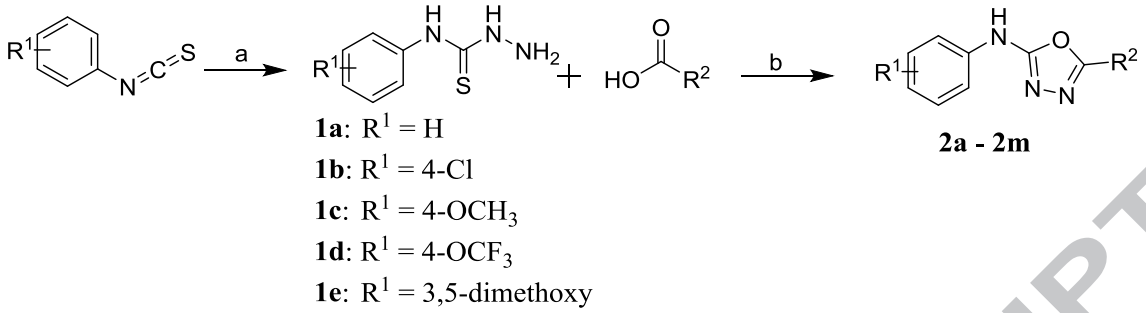

Scheme 1. Synthesis of 2-Anilino-1,3,4-oxadiazoles. Reagents and Conditions: (a) (1) N_2H_4, MeOH, rt, 1 h. (2) 65-80 ^oC, 20 min (88-96%); (b) EDCI (3 eq), CH_2Cl_2, rt, 12 h (50-84%). Structure of compounds **2a** – **2m** are listed in Table 1.

The synthesis of 1,2,4-oxadiazole derivatives started from commercially available nitriles that were reacted with hydroxylamine in EtOH/H_2O in the presence of $NaHCO_3$ to give the corresponding phenylamidoximes **3a**–**b** in good yields. The latter were suspended in DCM and then refluxed for 5 h in pyridine with ethyl chlorooxalate to provide 3-aryl-1,2,4-oxadiazole-5-carboxylates **4a**–**b**. Then , the obtained esters were eadily converted into the desired compounds **5a-c** by reaction with 3-substituted amine-1-yl propan-1-amine (Scheme 2).

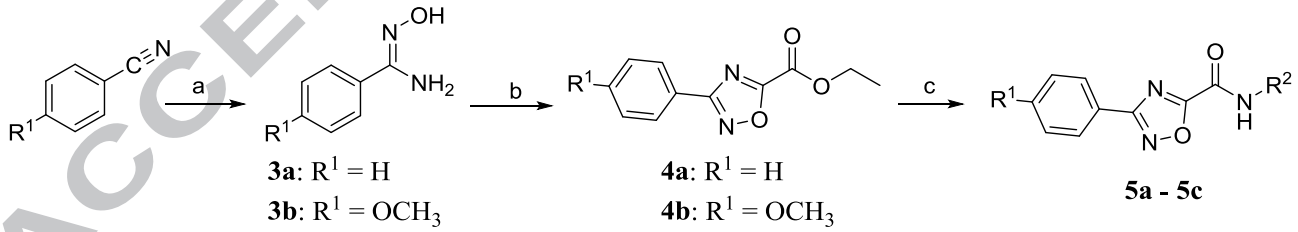

Scheme 2. Synthesis of 3-phenyl-1,2,4-oxadiazole derivatives. Reagents and Conditions: (a) NH_4OH, EtOH, $NaHCO_3$, reflux, 3 h (67-77%); (b) $CHCl_3$, ethyl chlorooxalate, rt for 30 min, then refluxed for 5 h (79-82%); (c) EtOH, alkyl amine, reflux for 8 h (73-87%). Structure of compounds **5a** – **5c** are listed in Table 1.

The synthesis of 5-methyl thiazole analogues (**7 - 36**) was based on literature procedure where the aryl / heteroaryl nitrile, α-mercaptocarboxylic acid, and pyridine were reacted to form the corresponding hydroxymethylthiazole (**6**).[41] Subsequently, the hydroxymethiazole was *O*-alkylated following a Williamson-type etherification

with K_2CO_3 as the base to afford the final compounds (**7 – 36**) (Scheme 3). Analogues **39-42** were synthesized by first refluxing 4-hydroxythiazole with 4 equivalents of α,α′-dibromo-*p*-xylene in acetone and K_2CO_3. After column chromatography, the monoether products (**38a-b**) were reacted with either piperidine or pyrrolidine to furnish the corresponding final compounds (**39-42**) (Scheme 4). The 5-ethyl thiazole analogues (**44-46**) were synthesized by first mixing the corresponding phenylthioamide, ethyl 2-bromobutanoate and pyridine under argon and slowly heating up to 100-110 °C for 2 h to form hydroxyethylthiazole (**43**), which was *O*-alkylated to afford the final compounds (**44 – 46**) (Scheme 5).[42]

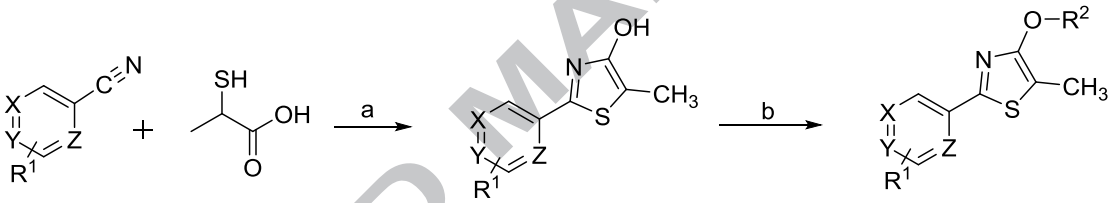

6a: R^1 = H; X= CH; Y = CH; Z = CH **7 - 37**
6b: R^1 = 4-Cl; X= CH; Y = CH; Z = CH
6c: R^1 = 4-CN; X= CH; Y = CH; Z = CH
6d: R^1 = 3-Cl; X= CH; Y = CH; Z = CH
6e: R^1 = H; X= CH; Y = N; Z = CH
6f: R^1 = H; X= N; Y = CH; Z = N

Scheme 3. Synthesis of 5-methyl thiazole derivatives. Reagents and Conditions: (a) pyridine, 100 ^oC for 2 h (69-96%); (b) DMF (or acetone), Cs_2CO_3 (or K_2CO_3) (3.0 eq.), KI (1.0 eq.), alkyl halide (0.9 eq.) (57-95%). Structure of compounds **7** – **37** are listed in Table 2.

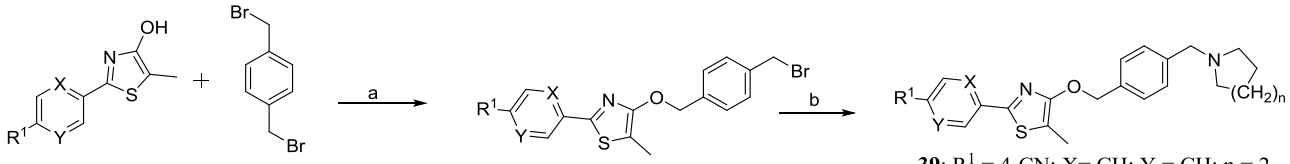

6c: R^1 = 4-CN; X= CH; Y = CH
6f: R^1 = H; X= N; Y = N

38a: R^1 = 4-CN; X= CH; Y = CH
38b: R^1 = H; X= N; Y = N

39: R^1 = 4-CN; X= CH; Y = CH; n = 2
40: R^1 = 4-CN; X= CH; Y = CH; n = 1
41: R^1 = H; X= N; Y = N; n = 2
42: R^1 = H; X= N; Y = N; n = 1

Scheme 4. Synthesis of xylene linker thiazole derivatives. Reagents and conditions: (a) K_2CO_3, acetone, reflux, 12 h (74-86%); (b) alicyclic amine, K_2CO_3, DMF, 60 ^oC, 12 h (84-90%).

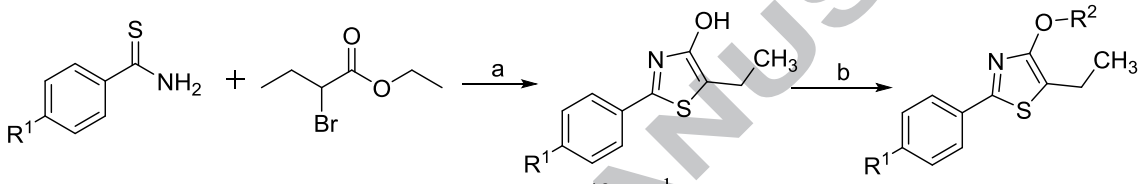

43a: R^1 = H
43b: R^1 = Cl

44 - 46

Scheme 5. Synthesis of 5-ethyl thiazole derivatives. Reagents and Conditions: (a) pyridine (1.0 eq.), 100-110 ^oC, 3 h (76-98%); (b) DMF, K_2CO_3 (3.0 eq.), KI (1.0 eq.), alkyl halide (0.9 eq.) (62-94%). Ligand structures of **44** – **46** are listed in Table 2.

2.3 Biological Evaluation

All final synthesized compounds were tested for their *in vitro* H_3R binding affinity in a binding assay by competitive displacement of [^{3}H]-N$^\alpha$-methylhistamine as radioligand. Their corresponding K_i values with 95% confidence intervals are listed in Table 1 and Table 2.

2.3.1 Oxadiazole-based ligands

As it was previously demonstrated that oxadiazoles, e.g. linked either via oxy-/thioethers or carboxamides to the basic amine moiety, are accepted as central core in H_3R ligands, a small series of 1,2,4- and 1,3,4-oxadiazole derivatives were designed.[38, 43]

Analogues of 1,3,4-oxadiazole scaffold showed low binding affinities at H_3R (K_i > 1000 nM), thus, permitting only limited conclusions for structural variations to improve H_3R affinity. The prototypes (**2a** - **2d**) without modifications at the anilino substructure resulted in ligand **2d** showing weak affinity. Only a few variations of these ligands were constructed to examine possibilities for improving this binding behavior, resulting in **2e** – **2m**. Ligands with alicyclic basic head and 2-3 carbon linkers showed comparable activity with **2d** exhibiting low micromolar K_i values (**2c** **2g**, **2j**, **2k**, and **2m**). However, analogues with the same linker length but rigid linker and basic head have negligible binding affinity (**2b**, **2f**, **2i**). This behavior implies the necessity of flexibility to position the basic head in favorable orientation for salt bridge formation with Asp114, described as crucial for H_3R antagonists/inverse agonists binding.[44] Moreover, ligands with noncyclic basic head and/or shorter linker (**2a**, **2h**, **2l**) appeared inactive, except the 4-chlorine derivative showing micromolar affinity (**2e**). These data suggest the need of a defined distance between the central core and the cyclic basic head for these compounds. Nevertheless, the modifications performed here were not able to improve affinity substantially, limiting any SAR interpretations in this series.

The smaller series of 1,2,4-oxadiazole-5-carboxamides analogues structurally related to previously described compounds FUB 654, ST-1095 or GSK247246were inactive (**5a**, **5b** and **5c**, Table 1).[33, 38, 39]Therefore, they are considered as unsuitable fundamental structure for further synthetic efforts, compared to 1,2,4-oxadiazole FUB 654 (Figure 2), anon-imidazole analogue of the highly affine Glaxo Wellcome compound GR175737 (K_i = 2.5 nM).[33, 45]Compared to previously published more potent alkyl-/thioether-linked oxadiazole derivatives (Figure 2),[38] *N*-phenyl-1,3,4-oxadiazole-2-amines and 1,2,4-oxadiazole-5-carboxamides seem to bear a less

promising or more restricted core motif on substitution and linkage, respectively. Subsequently, the more promising thiazole class has been followed in more detail.

Table 1. Oxadiazole-based ligands along with H_3R binding affinities.

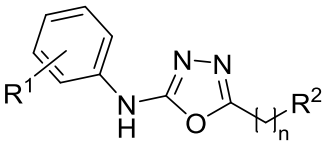

I

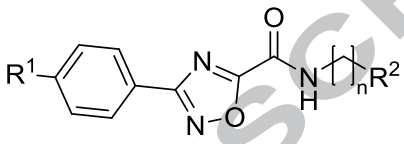

II

Compd No.	Scaffold	R^1	n	R^2	H_3R K_i (nM)[a] [95% CI][a]; (n)[b]
2a	I	H	3		> 5,000; (3)
2b	I	H	0	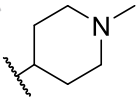	> 5,000; (2)
2c	I	H	2	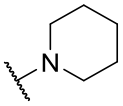	2,000 [100; 72,200]; (2)
2d	I	H	3	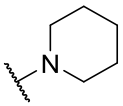	1,300 [700; 2,500]; (2)
2e	I	4-Cl	3		5,700 [300; 112,800]; (3)
2f	I	4-Cl	0	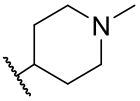	> 5,000; (2)
2g	I	4-Cl	2	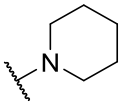	1,600 [100; 55,200]; (2)
2h	I	4-OCH_3	1		> 5,000; (2)
2i	I	4-OCH_3	0	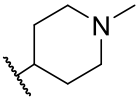	> 5,000; (2)
2j	I	4-OCH_3	2	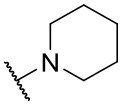	1,600 [700; 3,800]; (2)
2k	I	4-OCF_3	2	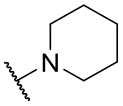	1,300 [100; 34,800]; (2)

2l	I	3,5-dimethoxy	1		> 5,000 (2)
2m	I	3,5-dimethoxy	2	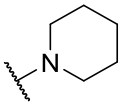	1,100 [1,000; 1,200]; (2)
5a	II	H	3	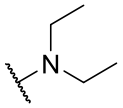	> 5,000 (2)
5b	II	H	3	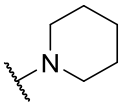	> 5,000 (4)
5c	II	OCH_3	3	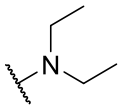	> 5,000; (2)

[a]Binding affinity values (K_i) are expressed as mean with 95% confidence intervals;
[b]Number of experiments.

2.3.2 Thiazole-based ligands

The synthetic approach for thiazole-based ligands was supported by the previously published structure, ST-979 (Figure 1).[37] They can be considered as analogues were the substituents were shifted by one carbon atom yielding **11** as initial structure with moderate affinity. The resulting analogues exhibited superior binding affinities with K_i values ranging from low micromolar to nanomolar concentrations. Similar to 1,3,4-oxadiazole analogues, optimum binding activities are achieved with pyrrolidine or piperidine basic heads. For example, compound **21** with pyrrolidine basic head and three-carbon chain linker demonstrated a K_i value of 4 nM. Yet, analogues with *para*-xylene (e.g., **41** and **42** with K_i values 7.0 nM and 72 nM, respectively) or piperidine carbamoyl (e.g., **14** , **20**, **23** with K_i values 5.4 nM, 54 nM and 42 nM, respectively) linkers showed high binding affinities. Interestingly, the methylpiperazine carbamoyl substituted thiazole **13** showed only weak affinity (K_i = 5,800 nM) compared to the piperidine carbamoyl linked analogue **14** being more active by more than three orders of magnitude. Different affinities of 2- and 3-carbon linked pyrrolidine or piperidine-analogues were detected between the corresponding structures of (pyrrolidine-1-

yl)alkoxy linked 2-phenylthiazoles with K_i of 47 nM and 520 nM for dimethylen **8** and trimethylen analogue **10**, respectively. Comparable binding behavior was detected between the corresponding 4-chlorophenylthiazole analogues **16** and **18** as well as between **17** and **19**, both carrying a (piperidin-1-yl)alkoxy linker instead (Table 2).The arbitrary region (i.e. the phenyl moiety) showed wide electronic and steric tolerability. Replacing the phenyl ring with pyridine was tolerable (or slightly less active) but not with pyrimidine (except when it is coupled with *para*-xylene linker in **41** and **42**). A cyano group in *para*-position generated the most active analogues (e.g., **21**, **22**), which may indicate the favorable positioning of hydrogen bond acceptor at this site presumably interacting with the Threonine residue identified by Roche et al.[46] Replacing the 5-methyl by an 5-ethyl substituent showed inconsistent pattern; it improves the binding affinity as with **46** (K_i = 200 nM), which is about five fold more active than its methyl counterpart (**19**, K_i = 930 nM)**,** but not with **44** and **45**.

Table 2. Thiazole-based ligands along with H_3R binding affinities.

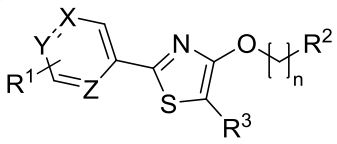

Compd No.	X	Y	Z	R^1	n	R^2	R^3	H_3R K_i [nM] [95% CI][a], (n)[b]
7	CH	CH	CH	H	3		CH_3	4,100 [1,400; 12,200]; (3)
8	CH	CH	CH	H	2	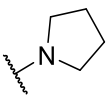	CH_3	47 [20; 110]; (3)
9	CH	CH	CH	H	2	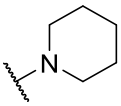	CH_3	200 [90; 490]; (3)
10	CH	CH	CH	H	3	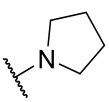	CH_3	520 [340; 780]; (3)
11	CH	CH	CH	H	3	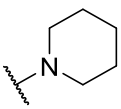	CH_3	870 [130; 5,710]; (5)

12	CH	CH	CH	H	1	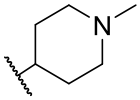	CH_3	220 [70; 650]; (8)
13	CH	CH	CH	H	0	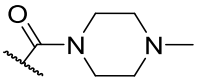	CH_3	5,800 [1,200; 27,000]; (4)
14	CH	CH	CH	H	0	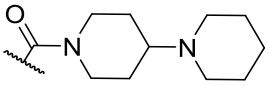	CH_3	5.4 [2.2; 13.2]; (3)
15	CH	CH	CH	4-Cl	3		CH_3	280 [70; 1,170]; (4)
16	CH	CH	CH	4-Cl	2	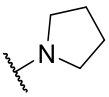	CH_3	22 [5; 98]; (3)
17	CH	CH	CH	4-Cl	2	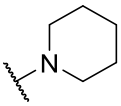	CH_3	44 [12; 167]; (3)
18	CH	CH	CH	4-Cl	3	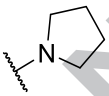	CH_3	450 [180; 1,150]; (3)
19	CH	CH	CH	4-Cl	3	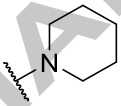	CH_3	930 [570; 1,540]; (4)
20	CH	CH	CH	4-Cl	0	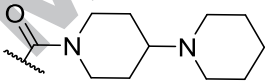	CH_3	54 [22; 131]; (3)
21	CH	CH	CH	4-CN	3	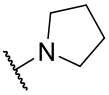	CH_3	4.2 [2.6; 6.6]; (3)
22	CH	CH	CH	4-CN	3	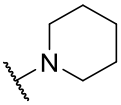	CH_3	21 [2; 201]; (3)
23	CH	CH	CH	4-CN	0	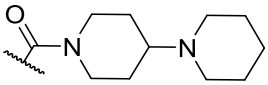	CH_3	42 [15; 122]; (4)
24	CH	CH	CH	3-Cl	2	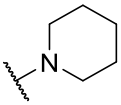	CH_3	600 [310; 1,150]; (3)
25	CH	CH	CH	3-Cl	3	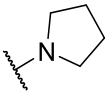	CH_3	430 [120; 1,550]; (3)
26	CH	CH	CH	3-Cl	3	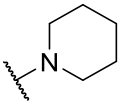	CH_3	300 [130; 700]; (4)
27	CH	CH	CH	3-Cl	0	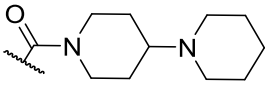	CH_3	98 [56; 170]; (6)
28	CH	N	CH	H	3		CH_3	110 [40; 300]; (4)
29	CH	N	CH	H	2	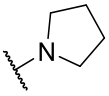	CH_3	100 [30; 380]; (4)

30	CH	N	CH	H	2	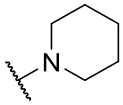	CH_3	57 [42; 78]; (3)
31	CH	N	CH	H	3	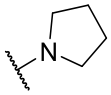	CH_3	410 [170; 1,010]; (4)
32	CH	N	CH	H	3	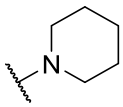	CH_3	130 [20; 820]; (3)
33	N	CH	N	H	3		CH_3	5,900 [2,800; 12,600]; (4)
34	N	CH	N	H	2	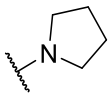	CH_3	2,100 [800; 6,100]; (4)
35	N	CH	N	H	3	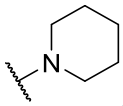	CH_3	1,100 [500; 2,400]; (6)
36	N	CH	N	H	0		CH_3	> 10,000
37	CH	CH	CH	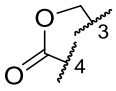	3	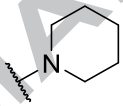	CH_3	87 [16; 462]; (5)
39	CH	CH	CH	4-CN	1	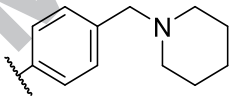	CH_3	450 [190; 1,100]; (4)
40	CH	CH	CH	4-CN	1	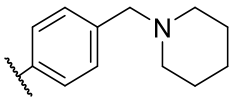	CH_3	190 [130; 280]; (3)
41	N	CH	N	H	1	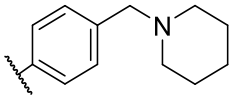	CH_3	7.0 [2.6; 18.4]; (4)
42	N	CH	N	H	1	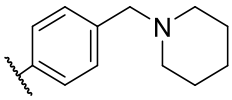	CH_3	72 [11; 492]; (4)
44	CH	CH	CH	H	3	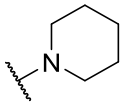	CH_2CH_3	380 [180; 810]; (3)
45	CH	CH	CH	4-Cl	3	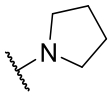	CH_2CH_3	170 [30; 870]; (4)
46	CH	CH	CH	4-Cl	3	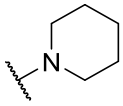	CH_2CH_3	200 [100; 370]; (4)

[a]Binding affinity values (K_i) are expressed as average along with 95% confidence intervals; [b]Number of experiments.

Accordingly, analogues combining optimum moieties, i.e. 4-cyanophenyl moiety as arbitrary region, *para*-xylene or piperidine carbamoyl linkers, and/or pyrrolidine or

piperidine basic heads were found to be the most active within this series of thiazole-based H_3R ligands.

2.6 *In silico* Molecular and ADMET properties of designed thiazole ligands.

Prediction of how much a ligand would have proper pharmacokinetics (ADME) and pharmacodynamics (e.g., toxicological) properties (drug-like) is of great importance during pre-clinical evaluation to assist drug discovery/development process, to guide the optimization from a lead compound to a successful drug candidate, and to reduce attrition rates during clinical trials, hence increasing the chance of reaching the market.[47]

Some important chemical descriptors correlate well with ADMET properties such as polar surface area (PSA) and low molecular weight (MW) for high oral absorption.[48] Likewise, rapid renal clearance is correlated with hydrophilic and small compounds. The hepatic metabolism of most drugs is associated with large and hydrophobic compounds. Higher lipophilicity of compounds leads to increased metabolism and poor absorption, along with an increased probability of binding to undesired hydrophobic macromolecules, thereby increasing the potential for toxicity.[49]

Table 3. Compliance of the most active ligands to Lipinski's and Veber's rules.

Compound	AlogP (< 5)	MW (< 500)	No. HBA[a] (≤ 10)	No. HBD[b] (≤ 5)	No. rotatable bonds (≤ 10)	Molecular PSA[c] (< 140 Å)
14	2.33	386.5	5	1	4	75
20	3.00	421.0	5	1	4	75
21	1.80	314.4	4	1	5	79
23	2.21	411.5	6	1	4	99
27	3.00	421.0	5	1	4	75
41	1.56	367.5	5	1	6	81

[a]Number of Hydrogen-bond acceptors (HBA); [b]Number of Hydrogen-bond donors (HBD); [c]Polar Surface Area (PSA).

Lipinski's[49] and Veber's[50] rules are one of the most important measures to evaluate the drug-likeness and to predict if a compound of certain chemical properties would be orally bioavailable. In spite of some observed exceptions to Lipinski's and Veber's rules, the vast majority (90%) of the orally bioavailable compounds are within their cut-off limits. Lipinski's rule of five states that, generally, an orally bioavailable compound should not violate the following criteria: ≤ 5 hydrogen bond donors (HBD); ≤ 10 hydrogen bond acceptors (HBA); MW < 500; and logP value of < 5. Alternatively, Veber's findings described the role of PSA and number of rotatable bonds as criteria to estimate the oral bioavailability. Veber's rule stated that for a compound to be orally bioavailable it should have either: a PSA ≤ 140 Å and ≤ 10 rotatable bonds, or ≤ 12 HBD and HBA in total and ≤ 10 rotatable bonds. Clearly from Table 3, the most potent ligands (those with K_i < 100 nM) followed all Lipinski's and Veber's rules without any exception, which highlight their drug-likeness properties and their potential to pass the drug development process.

The most active ligands were *in silico* screened for predicted pharmacokinetics properties (BBB penetration, absorption, solubility (Sw), hepatotoxicity, inhibition of CYP2D6, and plasma protein binding (PPB)) being summarized in Table 4. The intestinal absorption and BBB penetration were predicted by developing an ADME model using descriptors 2D PSA and AlogP98 that include 95% and 99% confidence ellipses. These ellipses define regions where well-absorbed compounds are expected to be found. All active ligands showed medium (brain-blood ratio between 0.3:1 and 1:1) to high (brain-blood ratio between 1:1 and 5:1) penetration of BBB and good intestinal absorption (at least 90% absorbed into bloodstream) within 95% confidence ellipses (Table 4 and Figure 3). These results are therapeutically crucial for H_3R ligands to be effective for targeting neurodegenerative diseases and their potential for

oral administration. Moreover, these ligands showed low (-6.0 < logSw < -4.0) to good (-4.0 < logSw < -2.0) solubility, non-hepatotoxicity, and variable properties for inhibition of CYP2D6 and PPB (Table 4). However, the compounds with highest affinity in the series (**14**, **21** and **41**) provide some deficiencies regarding BBB permeability and display high PPB (PPB > 95% as with **14** and **41**).

Table 4. Predicted ADME profiles of the most active ligands.

Compound	BBB[a]	Absorption[b]	Solubility[c]	Hepatotoxicity[d]	CYP2D6[e]	PPB[f]
14	2	0	3	nontoxic	inhibitor	2 (> 95%)
20	1	0	2	nontoxic	non-inhibitor	0 (< 90%)
21	2	0	3	nontoxic	non-inhibitor	1 (> 90%)
23	2	0	3	nontoxic	non-inhibitor	0 (< 90%)
27	1	0	2	nontoxic	non-inhibitor	0 (< 90%)
41	2	0	3	nontoxic	non-inhibitor	2 (> 95%)

[a]Predicts ability of the compound to penetrate the blood brain barrier (BBB). Levels 0, 1, 2, 3, or 4 correspond to very high, high, medium, low, or undefined penetration, respectively; [b]Predicts human intestinal absorption after oral administration. Levels 0, 1, 2, or 3 correspond to good, moderate, poor, or very poor absorption, respectively; [c]Predicts the solubility of each compound in water at 25°C. Levels 0, 1, 2, 3, 4, 5, or 6 correspond to extremely low, very low, low, good, optimal, too soluble, or unknown solubility, respectively; [d]Predicts the occurrence of dose-dependent human hepatotoxicity. [e]Predicts cytochrome P450, 2D6 inhibition. [f]Predicts the likelihood that a compound will be highly bound to carrier proteins on the blood (PPB, plasma protein binding). Levels 0, 1, or 2 correspond to binding < 90%, binding > 90%, or binding > 95%, respectively.

As ligand efficiency measures emerge as increasingly important parameters in hit-to-lead optimization, we calculated ligand efficiency (*LE*) and lipophilic ligand efficiency (*LLE*) according to literature, based on *in silico A*log*P*-values and *in vitro* binding affinities.[51] *LE* values were within the commonly accepted limits with *LE* > 0.3 kcal per mole per non-H-atoms (nHA) (0.42, 0.50 and 0.41 kcal / mole / nHA for compounds **14**, **21** and **41** respectively).[52] *LLE* values conform to the acceptance criteria of *LLE* > 5, being 5.9, 6.6 and 6.6 for **14**, **21** and **41**, respectively.[53]

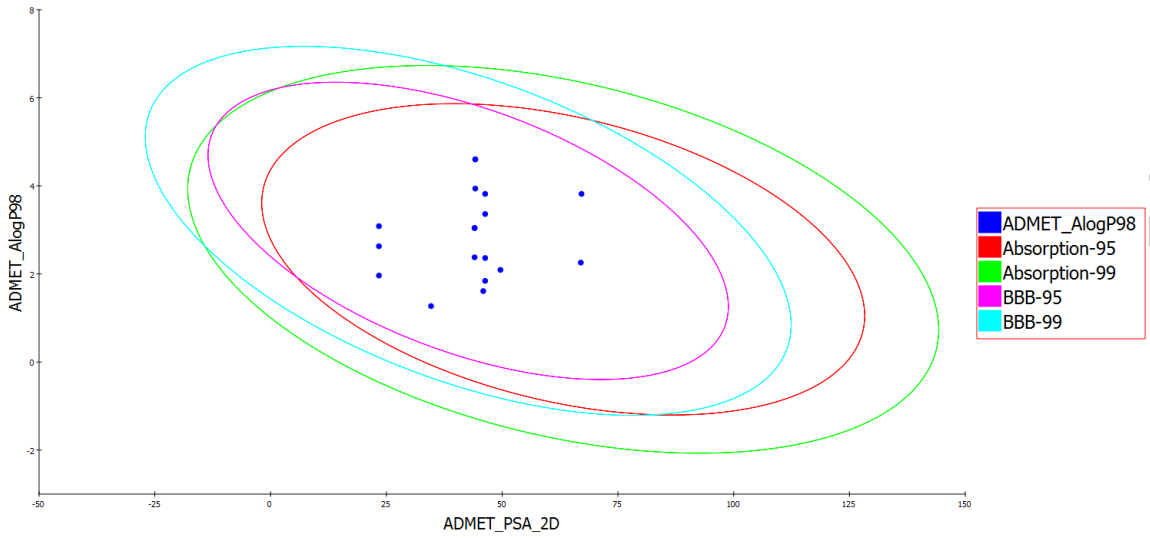

Figure 3. Plot of PSA vs AlogP (calculated via "Calculate Molecular Properties" module of Discovery Studio 2.5.5) for the most active ligands showing 95% and 99% confidence limit ellipses corresponding to penetration of BBB and intestinal absorption.

The United States Food and Drug Administration (US FDA) standard toxicity risk predictor software TOPKAT (Discovery Studio, Accelrys, USA) locates fragments within the compound that indicate a potential threat to toxicity risk. TOPKAT (TOxicity Prediction by Komputer Assisted Technology) employs robust and cross-validated Quantitative Structure Toxicity Relationship (QSTR) models for assessing various measures of toxicity and utilizing the patented Optimal Predictive Space validation method to assist in interpreting the results. Toxicity screening results of TOPKAT for the most active H_3R ligands showed no risk of AMES mutagenicity, and tolerable ocular and skin irritation (Table 5); however, they possess potential US FDA rodent carcinogenicity, except against female mouse. Compound **14** is the only non-skin sensitizing agent among the three most active compounds and appears as single-carcinogen in male mouse and female rat, whereas the cyano-containing ligands **21** and **41** differentiate as skin sensitizing and multi-carcinogenic agents. Moreover, particular attention was paid to the risk of aerobic biodegradability as 2-phenylthiazoles are known to produce hepatotoxic and/or nephrotoxic thioamides and

1,2-dicarbonyl-species upon oxidative metabolism.[54, 55] Thus, exclusively in 5-position alkylated thiazole derivatives were synthesized to achieve reduced oxidative ring-scission and biodegradable probability, confirmed by the TOPKAT screening results.[56]

Besides the biological evaluation, this *in silico* screening provided additional information that could be useful for further lead optimization of the presented compounds (cf. additional *in silico* ADMET and toxicity information on compounds **8**, **16**, **17**, **22**, **30**, **37,** and **42** is provided in Supplementary Material).

Table 5. Toxicity profile of the most active ligands using toxicity prediction, extensible protocol of Accelrys Discovery studio 2.5.5.

Compound	Aerobic BioDegradability[a]	AMES Mutagenicity[b]	Ocular Irritancy[c]	Skin Irritancy[c]	Skin Sensitizer[c]	Carcinogenicity_USFDA[d]			
						Female Mouse	Male Mouse	Female rat	Male Rat
14	-	-	+	-	-	-	+	+	-
20	-	-	+	-	-	-	-	-	-
21	-	-	+	-	++	-	+	++	++
23	-	-	+	-	-	-	+	++	++
27	-	-	+	-	-	-	-	-	-
41	-	-	+	+	++	+	+	+	++

[a]Prediction of oxidative degradability-properties of compounds. Indicators -, or + correspond to non-biodegradability, or degradability by bioorganisms, respectively; [b]Predicted mutagenicity in AMES mutagenicity test. Indicators -, or + correspond to non-mutagenicity, or mutagenicity, respectively; [c]Prediction of organic toxicity. Indicators -, +, or ++ correspond to none, mild, or severe / strong toxic properties, respectively; [d]Prediction of carcinogenic properties. Indicators -, +, or ++ correspond to classification as Non-Carcinogen, Single-Carcinogen, or Multi-Carcinogen, respectively.

3. Conclusions

A novel series of oxadiazole and thiazole derivatives as H_3R ligands are explored in the present study. Oxadiazole ligands showed mediocre affinities unlike the thiazole, which showed potent H_3R affinities in low nanomolar concentration range. The highest affinities are observed with ligands of pyrrolidine or piperidine basic heads and 2 – 3 carbon linkers. However, thiazole ligands of *para*-xylene or piperidine carbamoyl linkers showed high binding affinities, too. The examined compounds show excellent drug-like properties in compliance with Lipinski's and Veber's rules and satisfactory *in silico* ADMET properties. The results from this study will be helpful for further improvements of potent H_3R ligands.

4. Experimental

4.1. Chemistry

Reagents and solvents for synthesis were purchased from Sigma-Aldrich, VWR Chemicals, Fisher Scientific, Alfa Aesar and Chemsolute and were used without further purifications. ^{1}H-NMR and ^{13}C-NMR were recorded on a Bruker AMX spectrometer (Bruker, Germany) at 300 and 75 MHz respectively, where $CDCl_3$ or DMSO-d_6 was used as a solvent. Tetramethylsilane was used as standard and chemical shifts are reported in part per million (ppm). Spin multiplicities are given as s (singlet), d (doublet), dd (doublet of doublets), t (triplet), q (quintet) or m (multiplet). Approximate coupling constants (J) in Hertz (Hz). Number and assignment of protons (ax, axial; eq, equatorial; ph, phenyl; pip, piperidine; pyra, pyrazine; pyr, pyridine; pyrr, pyrrolidine). Elementary analyses (C, H, N) were measured on a CHN-Rapid (Heraeus, Germany) and all final compounds were within 0.4 % of the theoretical values. Electrospray ionization mass spectrometry (ESI-MS) was performed on an amaZon speed (Bruker, Germany) in positive polarity. Data are listed as mass number ([M+H$^+$]). High-resolution mass spectra (HRMS) were run in electrospray ionization (ESI) mode. Melting points (m.p., uncorrected) were determined on a M-564 Büchi melting point apparatus (Büchi, Germany). Preparative column chromatography was performed on silica gel 60 M, 0.04-0.063 mm (Macherey-Nagel, Germany) and thin-layer chromatography (TLC) was carried out using pre-coated silica gel 60 with fluorescence indicator at UV 254 nm (Macherey-Nagel, Germany).

4.1.1. General Reaction Procedures.

General Procedure (A). Preparation of 4-Phenyl-3-thiosemicarbazide. The phenylisothiocyanate (30 mmol) was added, dropwise, over a period of 1 h to a stirred

solution of hydrazine (30 mmol) in methanol (8 mL) at 65-80 ^{o}C. The reaction mixture was stirred for 20 min more at the same temperature. The solvent was removed by evaporation *in vacuo* and the precipitate was collected by filtration and washed with petroleum ether. The compound was used without further purification.

General Procedure (B). Preparation of 2-Anilino-5-alkyl-1,3,4-oxadiazole. A carboxylic acid (0.33 mmol), a 4-phenyl-3-thiosemicarbazide (0.33 mmol), and EDCI (182 mg, 1.0 mmol) were mixed in CH_2Cl_2 (15 mL), and the reaction mixture was stirred at room temperature for 12 h. The organic layer was washed three times with saturated $NaHCO_3$, dried over $MgSO_4$, filtered, and concentrated. Chromatography (5:95 MeOH/DCM, silica gel) of the residue afforded the title compound.

General Procedure (C). Preparation of Phenyl amidoximes. To a stirred solution of phenyl nitrile (0.1 mol) in ethanol (100 mL), a solution of hydroxylamine (0,6 mol) in H_2O (150 mL) was slowly added followed by $NaHCO_3$ (0.3 mol). The resulting mixture was refluxed for 3h. The solvent was evaporated *in vacuo* and the resulting residue was poured into cold water. The formed precipitate was filtered off, washed with water and dried *in vacuo*. The obtained product was recrystallized from methanol.

General Procedure (D). Preparation of 1,2,4-Oxadiazole-5-carboxylates. Pyridine (0.015 mol) was added to a solution of phenyl amidoxime (0.01 mol) dissolved in dry $CHCl_3$ (100 ml). Ethyl chloroxalate (0.025 mol) was then added to the solution under vigorous stirring. The mixture was stirred at room temperature for 30 min, then refluxed for 5 h, cooled to rt, washed with water and HCl (5%). Organic layer was dried under MgSO4, concentrated *in vacuo* and the formed residue was purified by flash-chromatography on silica gel.

General Procedure (E). Preparation of 1,2,4-Oxadiazole-5-carboxamides. A primary amine (0.5 mmol.) was added to the carboxylate (0.5 mmol) dissolved in dry ethanol (5 mL). The reaction mixture was refluxed for 12 h, and then cooled to rt. The organic solvent was dried *in vacuo* and the crude product was purified by flash-chromatography on silica gel to give the target compounds

General Procedure (F). Preparation of 4-Hydroxy-5-methylthiazole. Pyridine (0.005 mol) was added to a mixture of thiolactic acid (0.02 mol) and nitrile (0.0.2 mol) at 23 ^{O}C under argon. The reaction mixture was then heated at 100 ^{O}C for 2 h. After cooling, the precipitate was collected, washed with absolute ethanol, and recrystallized from methanol to afford the product.

General procedure (G). *O*-Alkylations of Hydroxy thiazoles

To a solution of thiazole (1.0 eq.) dissolved in DMF (4 mL), K_2CO_3 (3.0 eq.) was added, and the reaction mixture was left for 30 min at 60 °C. Then KI (1.0 eq.) and the alkyl halide (0.9 eq.) was added and the reaction was left for an additional 8 h. The reaction mixture was taken up in DCM, washed with Na_2CO_3 (3x) and dried over MgSO4 and concentrated *in vacuo*. The concentrate was purified by flash chromatography yielding the desired compound.

General procedure (H). Preparation of 2-Phenyl-4-hydroxy-5-ethylthiazole. Pyridine (5.83 mmol) was added to a mixture of ethyl 2-bromobutanoate (6.41 mmol) and thiobenzamide (5.83 mmol) at 23 ^{O}C under argon. The reaction mixture was then heated at 100 ^{O}C for 2 h. After cooling, the precipitate was collected and washed with absolute ethanol, and the recrystallized from methanol to afford the desired product.

General procedure (I). Preparation of Bromoethyl benzyl thiazole. 1,4-Bis(bromomethyl)benzen (4.0 mmol), 4-hydroxythiazole (1.0 mmol) and K_2CO_3 (2.0 mmol) dissolved in 50 mL acetone was refluxed for 12 h. After cooling, acetone was

evaporated and the crude product was constituted in DCM. The organic layer was washed with $NaHCO_3$ solution (3x) and dried over Na_2SO_3. The final compound was purified with flash chromatography.

General procedure (J). Nucleophilic substitution of Bromoethyl benzyl thiazole. The bromoethyl benzyl thiazole (1.0 eq.) was dissolved in DMF (4 mL) and K_2CO_3 (3.0 eq.) was added. The reaction mixture was left for 30 min at 60 °C, then the piperidine or pyrolidine (0.9 eq.) was added and the reaction was left for an additional 8 h. The reaction mixture was taken up in DCM, washed with Na_2CO_3 (3x) and dried over $MgSO_4$ and concentrated *in vacuo*. The concentrate was purified by flash chromatography yielding the desired compound.

5-Methyl-2-phenyl-4-(2-(pyrrolidin-1-yl)ethoxy)thiazole (8). Compound **8** was prepared according to procedure G from 5-methyl-2-phenylthiazol-4-ol and 1-(2-chloroethyl)pyrrolidine to afford 62 mg of yellow solid (70%). ^{1}H NMR ($CDCl_3$, 300 MHz) δ 7.77 (dd, *J* = 8.1, 1.8 Hz, 2H, ph-2,6*H*), 7.38 – 7.23 (m, 3H, ph-3,4,5*H*), 4.45 (t, *J* = 6.0 Hz, 2H, OCH_2), 2.87 (t, *J* = 6.0 Hz, 2H, OCH_2CH_2N), 2.73 – 2.50 (m, 4H, pyrr-2,5H_2), 2.22 (s, 3H, CH_3), 1.77 (p, *J* = 1.8 Hz, 4H, pyrr-3,4H_2). ^{13}C NMR (151 MHz, $CDCl_3$) δ 9.40, 23.53, 54.67, 55.32, 69.26, 107.09, 125.34, 128.78, 129.29, 134.00, 159.47, 159.53. HRMS *m*/*z* 289.1384 [$M+H^+$] (calcd for $C_{16}H_{21}N_2OS$, 289.1375). Anal. Calcd for $C_{16}H_{20}N_2OS$: C 66.63, H 6.99, N 9.51, S 11.12. Found: C 66.82, H 7.24, N 9.18, S 11.51.

5-Methyl-2-phenylthiazol-4-yl [1,4'-bipiperidine]-1'-carboxylate (14). Compound **14** was prepared according to procedure G from 5-methyl-2-phenylthiazol-4-ol and [1,4'-bipiperidine]-1'-carbonyl chloride to afford 74 mg of yellow solid (80%). ^{1}H NMR ($CDCl_3$, 300 MHz) δ 7.79 – 7.74 (dd, *J* = 2.1, 1.8 Hz,, 2H, ph-2,6*H*), 7.31 (d, *J*

= 1.8 Hz, 1H, ph-4*H*), 7.29 (d, *J* = 2.1 Hz, 2H, ph-3,5*H*), 4.27 (dd, *J* = 30.2, 12.8 Hz, 2H, pip^1-2,6H_{eq}), 2.85 (m, 2H, pip^1-2,6H_{ax}), 2.55 – 2.32 (m, 5H, pip^1-4*H*, pip^2-2,6$H_{2ax/eq}$), 2.22 (s, 3H, CH_3), 1.94 – 1.72 (m, 2H, pip^1-3,5H_{eq}), 1.67 – 1.42 (m, 6H, pip^1-3,5H_{ax}, pip^2-3,5$H_{2ax/eq}$), 1.42 – 1.27 (m, 2H, pip^2-4$H_{2ax/eq}$). ^{13}C NMR (75 MHz, $CDCl_3$) δ 10.03, 24.63, 26.21, 28.10, 44.40, 50.20, 62.36, 117.88, 125.72, 128.76, 129.81, 133.37, 151.79, 152.31, 161.20. HRMS *m*/*z* 386.1910 [M+H$^+$] (calcd for $C_{21}H_{28}N_3O_2S$, 386.1902). Anal. Calcd for $C_{21}H_{27}N_3O_2S$: C 65.43, H 7.06, N 10.90, S 8.32. Found: C 66.18, H 7.12, N 10.84, S 8.38.

2-(4-Chlorophenyl)-5-methyl-4-(2-(pyrrolidin-1-yl)ethoxy)thiazole (16). Compound **16** was prepared according to procedure G from 2-(4-chlorophenyl)-5-methylthiazol-4-ol and 1-(2-chloroethyl)pyrrolidine to afford 79 mg of yellow solid (91%). ^{1}H NMR ($CDCl_3$, 300 MHz) δ 7.66 (d, *J* = 8.6 Hz, 2H, ph-2,6*H*), 7.24 (d, *J* = 8.6 Hz, 2H, ph-3,5*H*), 4.40 (t, *J* = 6.0 Hz, 2H, OCH_2), 2.81 (t, *J* = 6.0 Hz, 2H, OCH_2CH_2N), 2.63 – 2.47 (m, 4H, pyrr-2,5H_2), 2.19 (s, 3H, CH_3), 1.72 (p, *J* = 3.0 Hz, 4H, pyrr-3,4H_2). ^{13}C NMR (75 MHz, DMSO) δ 9.28, 23.42, 54.59, 55.26, 69.42, 107.31, 126.37, 128.82, 132.38, 134.89, 157.85, 159.64. HRMS *m*/*z* 323.0991 [M+H$^+$] (calcd for $C_{16}H_{19}ClN_2OS$, 323.0985). Anal. Calcd for $C_{16}H_{20}ClN_2OS$: C 59.52, H 5.93, N 8.68, S 9.93. Found: C 59.88, H 6.07, N 8.41, S 10.37.

2-(4-Chlorophenyl)-5-methyl-4-(2-(piperidin-1-yl)ethoxy)thiazole (17). Compound **17** was prepared according to procedure G from 2-(4-chlorophenyl)-5-methylthiazol-4-ol and 1-(3-chloroethyl)piperidine to afford 43 mg of yellow solid (57%). ^{1}H NMR ($CDCl_3$, 300 MHz) δ 7.69 (d, *J* = 8.5 Hz, 2H, ph-2,6*H*), 7.28 (d, *J* = 8.5 Hz, 2H, ph-3,5*H*), 4.44 (t, *J* = 6.0 Hz, 3H, OCH_2), 2.76 (t, *J* = 6.0 Hz, 3H, OCH_2CH_2N), 2.62 – 2.47 (m, 4H, pip-2,6$H_{2ax/eq}$), 2.21 (s, 3H, CH_3), 1.72 – 1.52 (m, 4H, pip-3,5$H_{2ax/eq}$),

1.45 – 1.32 (m, 2H, pip-4$H_{2ax/eq}$). ^{13}C NMR (75 MHz, $CDCl_3$) δ, 9.73, 24.63, 26.34, 55.33, 58.66, 68.65, 107.37, 126.48, 128.93, 132.48, 134.99, 158.01, 159.78. HRMS *m*/*z* 337.1148 [M+H$^+$] (calcd for $C_{17}H_{22}ClN_2OS$, 337.1141). Anal. Calcd for $C_{17}H_{21}ClN_2OS$: C 60.61, H 6.28, N 8.32, S 9.52. Found: C 61.08, H 6.51, N 8.41, S 9.85.

2-(4-Chlorophenyl)-5-methylthiazol-4-yl [1,4'-bipiperidine]-1'-carboxylate (20). Compound **20** was prepared according to procedure G from 2-(3-chlorophenyl)-5-methylthiazol-4-ol and [1,4'-bipiperidine]-1'-carbonyl chloride to afford 84 mg of yellow solid (89%). ^{1}H NMR ($CDCl_3$, 300 MHz) δ 7.69 (d, *J* = 8.6 Hz, 2H, ph-2,6*H*), 7.27 (d, *J* = 8.6 Hz, 2H, ph-3,5*H*), 4.27 (dd, *J* = 28.1, 13.3 Hz, 2H, pip^1-2,6H_{eq}), 2.86 (m, 2H, pip^2-2,6H_{eq}), 2.62 – 2.34 (m, 5H, pip^1-4*H*, pip^2-2,6$H_{2ax/eq}$), 2.22 (s, 3H, CH_3), 1.96 – 1.74 (m, 2H, pip^1-3,5H_{eq}), 1.68 – 1.45 (m, 6H, pip^1-3,5H_{ax}, pip^2-3,5$H_{2ax/eq}$), 1.44 – 1.29 (m, 2H, pip^2-4H_2). ^{13}C NMR (75 MHz, $CDCl_3$) δ 10.02, 24.46, 25.96, 27.40, 27.97, 44.04, 44.33, 50.16, 62.39, 118.40, 126.90, 128.99, 131.86, 135.69, 151.88, 152.22, 159.79. HRMS *m*/*z* 420.1514 [M+H$^+$] (calcd for $C_{21}H_{26}ClN_3O_2S$, 420.1513). Anal. Calcd for $C_{21}H_{27}ClN_3O_2S$: C 60.06, H 6.24, N 10.01, S 7.63. Found: C 60.12, H 6.20, N 10.18, S 7.66.

4-(5-Methyl-4-(2-(pyrrolidin-1-yl)ethoxy)thiazol-2-yl)benzonitrile (21). Compound **21** was prepared according to procedure G from 2-(3-cyanophenyl)-5-methylthiazol-4-ol and 1-(2-chloroethyl)pyrrolidine to afford 67 mg of yellow solid (80%). ^{1}H NMR ($CDCl_3$, 300 MHz) δ 7.74 (d, *J* = 8.7 Hz, 2H, ph-2,6*H*), 7.49 (d, *J* = 8.7 Hz, 2H, ph-3,5*H*), 4.38 (t, *J* = 5.4 Hz, 2H, OCH_2), 2.84 (t, *J* = 5.5 Hz, 2H, OCH_2CH_2N), 2.66 – 2.55 (m, 4H, pyrr-2,5H_2), 2.16 (s, 3H, CH_3), 1.80 – 1.64 (m, 4H,

pyrr-3,4H_2). ^{13}C NMR (75 MHz, $CDCl_3$) δ 9.36, 31.25, 36.37, 54.98, 68.92, 109.48, 111.85, 118.48, 125.35, 132.44, 137.43, 156.31, 160.10. HRMS *m/z* 314.1332 [M+H$^+$] (calcd for $C_{17}H_{20}N_3OS$, 314.1327). Anal. Calcd for $C_{17}H_{19}N_3OS$: C 66.03, H 6.46, N 12.83, S 9.79. Found: C 66.18, H 6.51, N 12.79, S 9.72.

4-(5-Methyl-4-(3-(piperidin-1-yl)propoxy)thiazol-2-yl)benzonitrile (22). Compound **22** was prepared according to procedure G from 2-(3-cyanophenyl)-5-methylthiazol-4-ol and 1-(3-chloropropyl)piperidine to afford 75 mg of yellow solid (83%). ^{1}H NMR ($CDCl_3$, 300 MHz) δ 7.81 (d, *J* = 8.7 Hz, 2H, ph-2,6*H*), 7.55 (d, *J* = 8.7 Hz, 2H, ph-3-5*H*), 4.29 (t, *J* = 6.4 Hz, 2H, OCH_2), 2.45 – 2.40 (m, 2H, OCH_2CH_2), 2.39 – 2.31 (m, 4H, pip-2,6$H_{2ax/eq}$), 2.21 (s, 3H, CH_3), 2.03 – 1.82 (m, 2H, $OCH_2CH_2CH_2N$), 1.68 – 1.48 (m, 4H, pip-3,5$H_{2ax/eq}$), 1.45 – 1.27 (m, 2H, pip-4$H_{2ax/eq}$). ^{13}C NMR (75 MHz, $CDCl_3$) δ 9.40, 24.31, 25.80, 26.97, 54.54, 55.91, 69.11, 109.34, 112.00, 118.62, 125.45, 132.53, 137.66, 156.33, 160.53. HRMS *m/z* 342.1645 [M+H$^+$] (calcd for $C_{19}H_{24}N_3OS$, 342.1640). Anal. Calcd for $C_{19}H_{23}N_3OS$: C 66.83, H 6.79, N 12.31, S 9.39. Found: C 66.79, H 6.80, N 12.31, S 9.44.

2-(4-Cyanophenyl)-5-methylthiazol-4-yl [1,4'-bipiperidine]-1'-carboxylate (23). Compound **23** was prepared according to procedure G from 4-(4-hydroxy-5-methylthiazol-2-yl)benzonitrile and [1,4'-bipiperidine]-1'-carbonyl chloride to afford 91 mg of yellow solid (91%). ^{1}H NMR ($CDCl_3$, 300 MHz) δ 7.85 (d, *J* = 8.7 Hz, 2H, ph-2,6*H*), 7.59 (d, *J* = 8.2 Hz, 2H, ph-3,5*H*), 4.26 (dd, *J* = 31.1, 13.0 Hz, 2H, pip^1-2,6H_{eq}), 2.84 (m, 2H, pip^2-2,6H_{eq}), 2.56 – 2.44 (m, 5H, pip^1-4*H*, pip^2-2,6$H_{2ax/eq}$), 2.26 (s, 3H, CH_3), 2.01 – 1.76 (m, 2H, pip^1-3,5H_{eq}), 1.66 – 1.47 (m, 6H, pip^1-3,5H_{ax}, pip^2-3,5$H_{2ax/eq}$), 1.45 – 1.30 (m, 2H, pip^2-4H_2). ^{13}C NMR (75 MHz, $CDCl_3$) δ 10.08, 24.41,

25.93, 27.41, 27.96, 44.03, 44.31, 50.13, 62.24, 112.75, 118.37, 120.43, 125.93, 132.55, 137.00, 152.02, 152.55, 158.24. HRMS *m/z* 411.1862 [M+H$^+$] (calcd for $C_{22}H_{27}N_4O_2S$, 411.1855). Anal. Calcd for $C_{22}H_{26}N_4O_2S$: C 64.37, H 6.38, N 13.65, S 7.81. Found: C 64.44, H 6.51, N 13.51, S 7.70.

2-(3-Chlorophenyl)-5-methylthiazol-4-yl [1,4'-bipiperidine]-1'-carboxylate (27). Compound **27** was prepared according to procedure G from 2-(3-chlorophenyl)-5-methylthiazol-4-ol and [1,4'-bipiperidine]-1'-carbonyl chloride to afford 85 mg of yellow solid (89%). ^{1}H NMR ($CDCl_3$, 300 MHz) δ 7.81 – 7.78 (m, 1H, ph-2*H*), 7.64 – 7.58 (m, 1H, ph-5*H*), 7.35 – 7.19 (m, 2H, ph-3,4*H*), 4.27 (dd, *J* = 29.0, 13.3 Hz, 2H, pip^1-2,6H_{eq}), 2.86 (m, 2H, pip^1-2,6H_{ax}), 2.54 – 2.34 (m, 5H, pip^1-4*H*, pip^2-2,6$H_{2ax/eq}$), 2.23 (s, 3H, CH_3), 1.72 – 1.94 (m, 2H, pip^1-3,5H_{eq}), 1.67 – 1.46 (m, 6H, pip^1-3,5H_{ax}, pip^2-3,5$H_{2ax/eq}$), 1.44 – 1.33 (m, 2H, pip^2-4H_2). ^{13}C NMR (75 MHz, $CDCl_3$) δ 10.05, 24.54, 26.08, 27.47, 28.03, 44.09, 44.38, 50.19, 62.36, 118.83, 123.79, 125.64, 129.70, 130.04, 134.90, 134.95, 151.99, 152.21, 159.37. HRMS *m/z* 420.1504 [M+H$^+$] (calcd for $C_{21}H_{27}ClN_3O_2S$, 420.1513). Anal. Calcd for $C_{21}H_{26}ClN_3O_2S$: C 60.06, H 6.24, N 10.01, S 7.63. Found: C 60.10, H 6.29, N 10.10, S 7.58.

5-Methyl-4-(2-(piperidin-1-yl)ethoxy)-2-(pyridin-4-yl)thiazole (30). Compound **30** was prepared according to procedure G from 5-methyl-2-(pyridin-4-yl)thiazol-4-ol and 1-(3-chloroethyl)piperidine to afford 78 mg of yellow solid (82%). ^{1}H NMR ($CDCl_3$, 300 MHz) δ 8.55 (dd, *J* = 4.6, 1.7 Hz, 2H, pyr-3,5*H*), 7.61 (dd, *J* = 4.6, 1.7 Hz, 2H, pyr-2,6*H*), 4.46 (t, *J* = 6.0 Hz, 2H, OCH_2), 2.75 (t, *J* = 6.0 Hz, 2H, OCH_2CH_2N), 2.58 – 2.44 (m, 4H, pip-2,6$H_{2ax/eq}$), 2.25 (s, 3H, CH_3), 1.69 – 1.52 (m, 4H, pip-3,5$H_{2ax/eq}$), 1.46 – 1.32 (m, 2H, pip-4$H_{2ax/eq}$). ^{13}C NMR (75 MHz, $CDCl_3$) δ 9.51, 24.01, 25.68, 54.87, 58.04, 68.07, 109.80, 119.04, 140.55, 150.42, 155.92,

160.37. HRMS *m/z* 304.1482 [M+H$^+$] (calcd for $C_{16}H_{22}N_3OS$, 304.1484). Anal. Calcd for $C_{16}H_{21}N_3OS$: C 63.33, H 6.98, N 13.85, S 10.57. Found: C 63.67, H 7.22, N 13.92, S 10.67.

5-(5-Methyl-4-(3-(piperidin-1-yl)propoxy)thiazol-2-yl)isobenzofuran-1(3H)-one (37). Compound **37** was prepared according to procedure G from 5-(4-hydroxy-5-methylthiazol-2-yl)isobenzofuran-1(3H)-one and 1-(3-chloropropyl)piperidine to afford 72 mg of yellow solid (84%). ^{1}H NMR ($CDCl_3$, 300 MHz) δ 7.92 – 7.85 (m, 2H, isobenzofuran-4,7*H*), 7.82 (dd, *J* = 8.1, 0.8 Hz, 1H, isobenzofuran-6*H*), 5.27 (s, 2H, isobenzofuran-3H_2), 4.33 (t, *J* = 6.3 Hz, 2H, OCH_2), 2.68 – 2.39 (m, 6H, $OCH_2CH_2CH_2N$, pip-2,6$H_{2ax/eq}$), 2.24 (s, 3H, CH_3), 2.09 – 1.89 (m, 2H, OCH_2CH_2), 1.70 – 1.52 (m, 4H, pip-3,5$H_{2ax/eq}$), 1.50 – 1.33 (m, 2H, pip-4$H_{2ax/eq}$). ^{13}C NMR (75 MHz, $CDCl_3$) δ 9.45, 23.98, 25.33, 26.59, 54.41, 55.84, 68.92, 69.55, 109.43, 118.37, 125.74, 126.15, 126.19, 139.17, 147.32, 156.86, 160.40, 170.53. HRMS *m/z* 373.1593 [M+H$^+$] (calcd for $C_{20}H_{25}N_2O_3S$, 373.1586). Anal. Calcd for $C_{20}H_{24}N_2O_3S$: C 64.49, H 6.49, N 7.52, O 12.89, S 8.61. Found: C 64.57, H 6.35, N 7.62, S 8.67.

5-Methyl-4-((4-(piperidin-1-ylmethyl)benzyl)oxy)-2-(pyrazin-2-yl)thiazole (41). Compound **41** was prepared according to procedure J from 4-((4-(bromomethyl)benzyl)oxy)-5-methyl-2-(pyrazin-2-yl)thiazole and piperidine to afford 91 mg of yellow solid (89%). ^{1}H NMR ($CDCl_3$, 300 MHz) δ 9.22 (d, *J* = 1.5 Hz, 1H, pyra-6*H*), 8.60 – 8.12 (m, 2H, pyra-3,4*H*), 7.34 (d, *J* = 8.1 Hz, 2H, ph-2,6*H*), 7.25 (d, *J* = 8.1 Hz, 2H, ph-3,5*H*), 5.33 (s, 2H, phCH_2O), 3.42 (s, 2H, phCH_2N), 2.36 – 2.27 (m, 4H, pip-2,6$H_{2ax/eq}$), 2.23 (s, 3H, CH_3), 1.56 – 1.42 (m, 4H, pip-3,5$H_{2ax/eq}$), 1.40 – 1.26 (m, 2H, pip-4$H_{2ax/eq}$). ^{13}C NMR (75 MHz, $CDCl_3$) δ 9.63, 24.23, 25.76, 54.37, 63.39, 72.04, 112.07, 127.90, 129.40, 136.17, 137.86, 140.81, 143.68, 144.16, 146.96,

156.57, 160.42. HRMS *m/z* 381.1758 [M+H$^+$] (calcd for $C_{21}H_{25}N_4OS$, 381.1749). Anal. Calcd for $C_{21}H_{24}N_4OS$: C 66.29, H 6.36, N 14.72, S 8.43. Found: C 66.37, H 6.35, N 14.62, S 8.67.

5-Methyl-2-(pyrazin-2-yl)-4-((4-(pyrrolidin-1-ylmethyl)benzyl)oxy)thiazole (42). Compound **42** was prepared according to procedure J from 4-((4-(bromomethyl)benzyl)oxy)-5-methyl-2-(pyrazin-2-yl)thiazole and pyrrolidine to afford 87 mg of yellow solid (84%). ^{1}H NMR ($CDCl_3$, 300 MHz) δ 9.21 (d, *J* = 1.5 Hz, 1H, pyra-4*H*), 8.42 (d, *J* = 2.6 Hz, 1H, pyra-6*H*), 8.38 (dd, *J* = 2.6, 1.5 Hz, 1H, pyra-3*H*), 7.37 (d, *J* = 8.4 Hz, 2H, , ph-2,6*H*), 7.32 (d, *J* = 8.4 Hz, 2H, ph-3,5*H*), 5.33 (s, 2H, phCH_2O), 3.66 (s, 2H, phCH_2N), 2.68 – 2.47 (m, 4H, pyrr-2,5*H*), 2.24 (s, 3H, CH_3), 1.85 – 1.58 (m, 4H, pyrr-3,4*H*). ^{13}C NMR (75 MHz, $CDCl_3$) δ 9.62, 23.36, 53.88, 59.88, 71.87, 112.08, 128.10, 129.33, 136.77, 137.02, 140.78, 143.68, 144.18, 146.92, 156.60, 160.32. HRMS *m/z* 367.1587 [M+H$^+$] (calcd for $C_{20}H_{23}N_4OS$, 367.1593). Anal. Calcd for $C_{20}H_{22}N_4OS$: C 65.55, H 6.05, N 15.29, S, 8.75. Found: C 65.67, H 6.11, N 15.32, S 8.67.

4.2. Pharmacology

4.2.1 [^{3}H]-N^α-Methylhistamine hH_3 receptor displacement assay

The procedure was performed as described previously with slight modification: In brief, membrane preparations (20 µg/well) of HEK-293 cells stably expressing the human H_3 receptor (hH3R) were incubated in a mixture of [^{3}H]-N^α-methylhistamine (2 nM; K_D=3.08 nM as determined by saturation binding experiments) and appropriate concentrations of the present competitors (seven to eleven concentrations between 0.01 nM and 10 µM) in 96-well microtiter plates with a final assay volume of 200 µl per well. Preparation of competitor-concentrations was carried out by serial

dilution of 10 mM and 3 mM stocks using a Freedom EVO pipetting instrument (TECAN®, Männedorf, Switzerland). For sample filtration ice-cold demineralized water was used. Specific binding was analyzed by non-linear squares fit via GraphPad-Prism™ (2012, vers. 6.01, La Jolla, CA, USA). Affinities (K_i) were calculated from IC_{50}-values using the Cheng-Prusoff correction and expressed as means from at least two independent experiments in triplicates within 95% confidence intervals.[57]

4.3 Molecular descriptor analysis

Molecular properties of most active ligands (those with K_i < 100 nM) were calculated using ‘‘Calculate Molecular Properties’’ module of Discovery Studio 2.5.5 client package (Accelrys, San Diego, USA). These descriptors include MW, number HBD and HBA, an octanol / water partition coefficient (log *P*), number of rotatable bonds, and molecular PSA.

4.4. ADME and Toxicity Studies

In silico ADME profiling for the most active ligands were measured using “ADMET Descriptors” module of Accelrys Discovery studio 2.5.5. The calculated ADME descriptors include BBB, intestinal absorption, solubility, hepatotoxicity, inhibition of CYP2D6, and plasma protein binding.

Toxicity profiling of the active ligands were conducted using TOPKAT toxicity estimation of Discovery Studio 2.5.5. TOPKAT computes a probable value of toxicity for a submitted chemical structure from a quantitative structure-toxicity relationship (QSTR) equation. The product of a structure descriptors and its corresponding coefficient is the descriptors contribution to the probable toxicity. Toxicity profile

involves screening for aerobic biodegradability, AMES (activity in the salmonella / mammalian microsome mutagenicity) mutagenicity, ocular and skin irritancy, skin sensitizer, and carcinogenicity.

Acknowledgements

This work was facilitated by the George Forster Research Fellowship, granted by the Alexander von Humboldt-Foundation (MAK). We thank Gina Alpert for the initial pharmacological screening of the present compounds. HEK-293 cells stably expressing the H_3R were a kind gift of Prof. Dr. Jean-Charles Schwartz (Bioprojet, France). Further parts of this work were supported by funding of the German Research Society (DFG INST 208/664-1 FUGG) and the EU COST action CA15135.

Supplementary material

Supplementary material associated with this article can be found, in the online version. These data include the analytical data of all compounds synthesized in this study.

References

1. Hu W, Chen Z. The roles of histamine and its receptor ligands in central nervous system disorders: An update. *Pharmacol Ther*. 2017;175:116-132.
2. Nieto-Alamilla G, Márquez-Gómez R, García-Gálvez A-M, et al. The Histamine H3 Receptor: Structure, Pharmacology, and Function. *Mol Pharmacol*. 2016;90:649-673.
3. Panula P, Nuutinen S. The histaminergic network in the brain: basic organization and role in disease. *Nat Rev Neurosci*. 2013;14:472.
4. Tiligada E, Kyriakidis K, Chazot PL, et al. Histamine pharmacology and new CNS drug targets. *CNS Neurosci Ther*. 2011;17:620-628.
5. Parsons ME, Ganellin CR. Histamine and its receptors. *Br J Pharmacol*. 2006;147 Suppl 1:S127-135.
6. Panula P, Chazot PL, Cowart M, et al. International Union of Basic and Clinical Pharmacology. XCVIII. Histamine Receptors. *Pharmacol Rev*. 2015;67:601-655.
7. Arrang JM, Garbarg M, Schwartz JC. Auto-inhibition of brain histamine release mediated by a novel class (H3) of histamine receptor. *Nature*. 1983;302:832-837.
8. Schwartz JC, Arrang JM, Garbarg M, et al. Histaminergic transmission in the mammalian brain. *Physiol Rev*. 1991;71:1-51.
9. Singh M, Jadhav HR. Histamine H3 receptor function and ligands: recent developments. *Mini Rev Med Chem*. 2013;13:47-57.
10. Schlicker E, Fink K, Gothert M, et al. The pharmacological properties of the presynaptic serotonin autoreceptor in the pig brain cortex conform to the 5-HT1D receptor subtype. *Naunyn Schmiedebergs Arch Pharmacol*. 1989;340:45-51.
11. Schlicker E, Schunack W, Gothert M. Histamine H3 receptor-mediated inhibition of noradrenaline release in pig retina discs. *Naunyn Schmiedebergs Arch Pharmacol*. 1990;342:497-501.
12. Heron A, Rouleau A, Cochois V, et al. Expression analysis of the histamine H(3) receptor in developing rat tissues. *Mech Dev*. 2001;105:167-173.
13. Krementsov DN, Wall EH, Martin RA, et al. Histamine H(3) receptor integrates peripheral inflammatory signals in the neurogenic control of immune responses and autoimmune disease susceptibility. *PLoS One*. 2013;8:e62743.
14. Sharma HS, Skaper SD, Sharma A. Commentary: Histaminergic Drugs Could be Novel Targets for Neuroprotection in CNS Disorders. *CNS Neurol Disord Drug Targets*. 2016;15:642-643.
15. Khanfar MA, Affini A, Lutsenko K, et al. Multiple Targeting Approaches on Histamine H3 Receptor Antagonists. *Front Neurosci*. 2016;10:201.
16. Lin JS, Sergeeva OA, Haas HL. Histamine H3 receptors and sleep-wake regulation. *J Pharmacol Exp Ther*. 2011;336:17-23.
17. Raddatz R, Tao M, Hudkins RL. Histamine H3 antagonists for treatment of cognitive deficits in CNS diseases. *Curr Top Med Chem*. 2010;10:153-169.
18. Gemkow MJ, Davenport AJ, Harich S, et al. The histamine H3 receptor as a therapeutic drug target for CNS disorders. *Drug Discov Today*. 2009;14:509-515.
19. Esbenshade TA, Browman KE, Bitner RS, et al. The histamine H3 receptor: an attractive target for the treatment of cognitive disorders. *Br J Pharmacol*. 2008;154:1166-1181.

20. Łażewska D, Kieć-Kononowicz K. Progress in the development of histamine H3 receptor antagonists/inverse agonists: a patent review (2013-2017). *Expert Opin Ther Pat*. 2018;28:175-196.
21. Sander K, Kottke T, Stark H. Histamine H3 receptor antagonists go to clinics. *Biol Pharm Bull*. 2008;31:2163-2181.
22. Syed YY. Pitolisant: First Global Approval. *Drugs*. 2016;76:1313-1318.
23. Schwartz JC. The histamine H3 receptor: from discovery to clinical trials with pitolisant. *Br J Pharmacol*. 2011;163:713-721.
24. Longstreth WT, Jr., Koepsell TD, Ton TG, et al. The epidemiology of narcolepsy. *Sleep*. 2007;30:13-26.
25. Abad VC, Guilleminault C. New developments in the management of narcolepsy. *Nat Sci Sleep*. 2017;9:39-57.
26. Berlin M, Boyce CW, Ruiz Mde L. Histamine H3 receptor as a drug discovery target. *J Med Chem*. 2011;54:26-53.
27. Roche O, Nettekoven M, Vifian W, et al. Refinement of histamine H3 ligands pharmacophore model leads to a new class of potent and selective naphthalene inverse agonists. *Bioorg Med Chem Lett*. 2008;18:4377-4379.
28. Axe FU, Bembenek SD, Szalma S. Three-dimensional models of histamine H3 receptor antagonist complexes and their pharmacophore. *J Mol Graph Model*. 2006;24:456-464.
29. Wingen K, Stark H. Scaffold variations in amine warhead of histamine H(3) receptor antagonists. *Drug Discov Today Technol*. 2013;10:e483-489.
30. Schlegel B, Laggner C, Meier R, et al. Generation of a homology model of the human histamine H(3) receptor for ligand docking and pharmacophore-based screening. *J Comput Aided Mol Des*. 2007;21:437-453.
31. Saha R, Tanwar O, Marella A, et al. Recent updates on biological activities of oxadiazoles. *Mini Rev Med Chem*. 2013;13:1027-1046.
32. Chhabria MT, Patel S, Modi P, et al. Thiazole: A Review on Chemistry, Synthesis and Therapeutic Importance of its Derivatives. *Curr Top Med Chem*. 2016;16:2841-2862.
33. Meier G, Apelt J, Reichert U, et al. Influence of imidazole replacement in different structural classes of histamine H(3)-receptor antagonists. *Eur J Pharm Sci*. 2001;13:249-259.
34. Denonne F, Atienzar F, Celanire S, et al. Phenyl-oxazoles, a new family of inverse agonists at the H3 histamine receptor. *ChemMedChem*. 2010;5:206-212.
35. Frymarkiewicz A, Walczynski K. Non-imidazole histamine H3 ligands, part IV: SAR of 1-[2-thiazol-5-yl-(2-aminoethyl)]-4-n-propylpiperazine derivatives. *Eur J Med Chem*. 2009;44:1674-1681.
36. Guryn R, Staszewski M, Stasiak A, et al. Non-Imidazole Histamine H(3) Ligands. Part VII. Synthesis, In Vitro and In Vivo Characterization of 5-Substituted-2-thiazol-4-n-propylpiperazines. *Molecules*. 2018;23.
37. Walter M, von Coburg Y, Isensee K, et al. Azole derivatives as histamine H-3 receptor antagonists, Part I: Thiazol-2-yl ethers. *Bioorg Med Chem Lett*. 2010;20:5879-5882.
38. Walter M, Isensee K, Kottke T, et al. Azole derivatives as histamine H3 receptor antagonists, Part 2: C-C and C-S coupled heterocycles. *Bioorg Med Chem Lett*. 2010;20:5883-5886.

39. Wang R, Lu H, inventor; GlaxoSmithKline Intellectual Property Development Limited, assignee. Therapeutic uses. Patent WO2013107336. July 25, 2013.
40. Chen Y, Zhen W, Guo T, et al. Histamine Receptor 3 negatively regulates oligodendrocyte differentiation and remyelination. *PLoS One*. 2017;12:e0189380.
41. Kerdesky FA, Holms JH, Moore JL, et al. 4-hydroxythiazole inhibitors of 5-lipoxygenase. *J Med Chem*. 1991;34:2158-2165.
42. Badiola E, Fiser B, Gomez-Bengoa E, et al. Enantioselective construction of tetrasubstituted stereogenic carbons through Bronsted base catalyzed michael reactions: alpha'-hydroxy enones as key enoate equivalent. *J Am Chem Soc*. 2014;136:17869-17881.
43. Folmer J, Hunt SF, Hamley P, et al. Novel piperidine derivative for the treatment of depression, Google Patents, 2006.
44. Kuder KJ, Lazewska D, Kaleta M, et al. Synthesis and biological activity of novel tert-amylphenoxyalkyl (homo)piperidine derivatives as histamine H3R ligands. *Bioorg Med Chem*. 2017;25:2701-2712.
45. Clitherow JW, Beswick P, Irving WJ, et al. Novel 1, 2, 4-oxadiazoles as potent and selective histamine H3 receptor antagonists. *Bioorg Med Chem Lett*. 1996;6:833-838.
46. Roche O, Nettekoven M, Vifian W, et al. Refinement of histamine H3 ligands pharmacophore model leads to a new class of potent and selective naphthalene inverse agonists. *Bioorg Med Chem Lett*. 2008;18:4377-4379.
47. Meanwell NA. Improving drug candidates by design: a focus on physicochemical properties as a means of improving compound disposition and safety. *Chem Res Toxicol*. 2011;24:1420-1456.
48. Wessel MD, Jurs PC, Tolan JW, et al. Prediction of human intestinal absorption of drug compounds from molecular structure. *J Chem Inf Comput Sci*. 1998;38:726-735.
49. Lipinski CA, Lombardo F, Dominy BW, et al. Experimental and computational approaches to estimate solubility and permeability in drug discovery and development settings. *Adv Drug Deliv Rev*. 2001;46:3-26.
50. Veber DF, Johnson SR, Cheng HY, et al. Molecular properties that influence the oral bioavailability of drug candidates. *J Med Chem*. 2002;45:2615-2623.
51. Hopkins AL, Keseru GM, Leeson PD, et al. The role of ligand efficiency metrics in drug discovery. *Nat Rev Drug Discov*. 2014;13:105-121.
52. Hopkins AL, Groom CR, Alex A. Ligand efficiency: a useful metric for lead selection. *Drug Discov Today*. 2004;9:430-431.
53. Leeson PD, Springthorpe B. The influence of drug-like concepts on decision-making in medicinal chemistry. *Nat Rev Drug Discov*. 2007;6:881-890.
54. Mizutani T, Suzuki K. Relative hepatotoxicity of 2-(substituted phenyl)thiazoles and substituted thiobenzamides in mice: evidence for the involvement of thiobenzamides as ring cleavage metabolites in the hepatotoxicity of 2-phenylthiazoles. *Toxicol Lett*. 1996;85:101-105.
55. Mizutani T, Yoshida K, Kawazoe S. Possible role of thioformamide as a proximate toxicant in the nephrotoxicity of thiabendazole and related thiazoles in glutathione-depleted mice: structure-toxicity and metabolic studies. *Chem Res Toxicol*. 1993;6:174-179.
56. Kalgutkar AS, Gardner I, Obach RS, et al. A comprehensive listing of bioactivation pathways of organic functional groups. *Curr Drug Metab*. 2005;6:161-225.

57. Cheng Y, Prusoff WH. Relationship between the inhibition constant (K1) and the concentration of inhibitor which causes 50 per cent inhibition (I50) of an enzymatic reaction. *Biochem Pharmacol*. 1973;22:3099-3108.

Highlight Bullets

- Novel non-imidazole histamine H_3 receptor ligands based on different azole cores
- 1,3-Thiazoles superior binding properties to that of 1,2,4- and 1,3,4-oxadiazoles
- 2-Aryl-1,3-thiazoles optimized with histamine H3R amine warhead scaffolds
- Numerous different compounds with nanomolar binding affinities
- Favorable ADME and toxicity properties based on *in silico* profiling

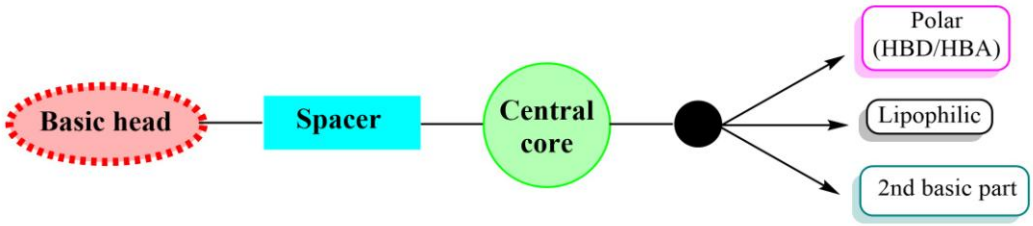

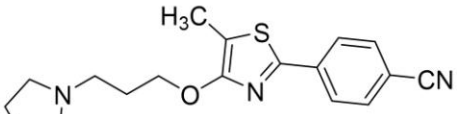

21, H_3R $K_i = 4$ nM

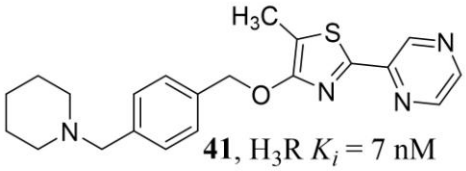

41, H_3R $K_i = 7$ nM